JOURNAL OF APPLIED ELECTROCHEMISTRY 25 (1995) 1091–1097

Electrodeposition of Ni–W–B amorphous alloys

N. ISAEV, J. G. OSTERYOUNG

Department of Chemistry, North Carolina State University, Raleigh, North Carolina, 27695-8204, USA

Received 17 August 1994

Partial polarization curves at the glassy carbon rotating disc electrode have been used to study the electrodeposition of Ni and Ni–W alloy from citrate-containing solution. For deposition of Ni–W alloys, the partial polarization curves indicate diffusion control for nickel reduction and stoichiometric limitation for tungsten deposition by the composition of the alloy. Plating experiments show that current efficiency of the electrodeposition and composition of the resulting alloy depend on the parameters of the electrolysis. The best conditions for electrodeposition of the alloy Ni–W–B are current density of 45–50 mA cm^{-2}, temperature of 60–70 °C, Ni(II) concentration of 20–25 mM, and pH 8.5. Pulsed galvanostatic plating at 1 Hz increased slightly the current efficiency. The concentration of Ni(II) in the solution can be self-regulated by using a nickel bipolar electrode in the cathode compartment.

1. Introduction

Amorphous metallic alloys became attractive in physics and engineering during the 1960s, when rapid quenching had become available as a relatively simple method of producing them [1]. At the same time methods were developed for producing amorphous metal films on substrates by electrochemical deposition from solution [2, 3]. Further methods for synthesis of amorphous materials emerged after that: ion implantation, evacuation and condensation on a cooled substrate, and sputtering with beams of inert gas ions. It was discovered recently that metallic alloys become amorphous at ultrahigh pressures [4]. The ability of amorphous alloys of iron group metals to passivate in aqueous solutions has been responsible for the enormous interest of corrosion scientists in these materials [5–7].

A number of papers have been dedicated to the electrodeposition of amorphous alloys [8]. Previous papers have dealt with anodic reactions of electrolytes for plating Co–W–B and Ni–W–B amorphous alloys [9] and with methods for characterizing the electroplating bath for electrodeposition of the Co–W–B alloy [10]. In addition, the anodic reactions of the cobalt-containing alloy have been investigated [11]. Cathodic reaction of the nickel alloy formation in citrate electrolytes were investigated by Wiart and coworkers [12, 13]. It has been shown that in acidic solution there is a strong interaction between discharged cations, and current efficiency depends on the electrolyte composition and on current density.

The present paper describes the results of an investigation of plating parameters for Ni–W–B alloys to find, in this complex system, the acceptable ranges of critical parameters. Under normal conditions intended to produce the amorphous alloy, the concentration of Ni(II) is easily depleted, which affects adversely the current efficiency and control of composition of the resulting plate. A particular goal of this work was, therefore, to find a method for self-regulation of the concentration of Ni(II) in the plating bath.

2. Experimental details

2.1. *Determination of Ni(II) in solution*

For determination of Ni(II) (in the solution) square-wave voltammetry (SWV) was used as implemented by an EG&G PARC 273 potentiostat with our own software through a PDP8e computer. The system is essentially the same as that with EG&G PARC 270 soft ware. The working electrode was an EG&G model 303A static mercury drop electrode. The parameter values were: step (ΔE) 10 mV, square wave amplitude (E_{sw}) 50 mV, frequency (f) 100 Hz, conditioning potential −0.8 V; conditioning time 1 s. Ten replicates were taken for each concentration of Ni(II). The medium was ammonia buffer of pH 9.6: 0.25 M NH_4OH and 0.25 M NH_4Cl.

The reduction of Ni(II) is totally irreversible under these conditions. Reduction of Ni(II) gave two net current peaks when the concentration of Ni(II) in the ammonia buffer was more than 1 mM. Consequently, the range of concentration 0.01–0.5 mM was chosen for a calibration curve.

2.2. *Cyclic and rotating disc voltammetry*

The potentiostat EG&G PARC 273 and ring disc electrode system EG&G PARC model 636 were used for all rotating disc experiments.

Working electrode was a commercial Pine AFDT 29SGCGC rotating disc (disc diam. 5.61 mm, inner ring diam. 6.25 mm, outer ring diam. 8.43 mm). The glassy carbon electrode was polished before each series of experiments by using a Microcloth polishing

0021-891X

cloth with suspensions of alumina powder down to 0.05 μm. The reference electrode here and for the determination of Ni(II) was saturated calomel (SCE) and all potentials are quoted with respect to this electrode.

The composition of the solution for the nickel deposition is as follows: sodium citrate 0.244 M; ammonium sulfate 0.417 M; nickel sulfate · $7H_2O$ 0.025 M; sodium lauryl sulfate 0.1 g. The pH was kept at 8.5 by means of NH_4OH. In the case of the Ni–W alloy deposition sodium tungstate (0.234 M) was added to the solution.

The procedure for obtaining partial polarization curves is as follows. First, nickel (or Ni–W alloy) was deposited chronoamperometrically to determine total current i_t

$$i_t = Q_t^c/t_c$$

where i_t is total cathodic current (mA), Q_t^c is total quantity of electricity passed through the cathode (C), and t_c the deposition time (s).

The nickel (or Ni–W alloy) was then dissolved chronoamperometrically in a known volume of ammonia buffer (10 m dm^3, 50 °C) for the determination of the current (i_d) for deposition of nickel (or Ni–W alloy)

$$i_d = Q^a/t_a$$

where i_d is current (mA) for nickel (or Ni–W alloy) deposition, Q^a is quantity of electricity for the dissolution of the deposit (C), t_a is the time of dissolution (s).

In the case of the nickel deposition, $i_d = i_{Ni}$, whereas in the case of the alloy deposition, $i_d = i_{Ni} + i_W$.

Square-wave voltammetry was used to determine the nickel deposition current (i_{Ni}) in the case of alloy deposition. This was done by measuring the concentration of nickel in solution resulting from electrodissolution of the alloy. The currents for hydrogen evolution and tungsten deposition were then calculated according to

$$i_H = i_t - i_d$$

$$i_W = i_d - i_{Ni}$$

Three replicates were taken for each potential.

2.3. *Plating experiments (Ni–W–B alloy)*

The composition of the plating bath is (per litre): sodium citrate 63 g (0.244 M); sodium tungstate 69 g (0.234 M); boron phosphate 5 g (45.5 mM); nickel sulfate · $7H_2O$ 6.6 g (23.6 mM); ammonium sulfate 55 g (0.417 M); sodium lauryl sulfate 0.1 g. The pH was kept at 8.5 by means of NH_4OH.

Both a steel cell (0.075 dm^3) and glass cell (2 dm^3) were used.

Cathodes of copper or platinum wire or foil were used. The steel cell body was used as an anode. An anode chamber separated from the cathode by a Nafion® membrane was used with the glass cell.

For determination of nickel in the bath solution and in the deposits, the SWV technique was used. For determination of Ni(II), 1 m dm^3 of the bath solution was diluted in the ammonia buffer. To determine nickel in the deposit, the Ni–W–B alloy deposit was weighed and then anodically dissolved in the ammonia buffer in the course of 1–2 h (anode current density was 10 mA cm^{-2}). Subsequently, this solution was analysed by SWV. The quantity of electricity equivalent to the weight of deposit was calculated by using the mass of the deposit (m) and the Faraday law:

$$Q_1 = m/g_a$$

where g_a is the electrochemical equivalent weight of the alloy. The equivalent weight of the deposit is related to the composition by

$$g_a = g_{Ni}x_{Ni} + g_W x_W$$

where x refers to mole fraction. Here $g_{Ni} = 0.304\,\text{mg C}^{-1}$ and $g_W = 0.317\,\text{mg C}^{-1}$. The quantity of electricity in the experiment was calculated as

$$Q_2 = It$$

where I is the current (A) and t is the duration of the electrolysis (s). The current efficiency was determined as the ratio Q_1/Q_2. Previous analysis of Ni–W–B deposits suggested a constant boron content no greater than 1% [14]. Thus the mole fraction of W in the deposit was determined as

$$x_W = (1 - 0.01 - x_{Ni})$$

The mole fraction (x) of tungsten is related to the weight fraction (w) by

$$w_W = \frac{x_W A_W}{x_W A_W + x_{Ni} A_{Ni} + x_B A_B}$$

where A is atomic weight of the element. Thus a mole ratio of

$$\frac{x_{Ni}}{x_W} = \frac{A_W}{A_{Ni}} \times \frac{w_{Ni}}{w_W} = 3.13\frac{w_{Ni}}{w_W}$$

corresponds to a weight fraction of nickel of

$$w_{Ni} = w_W 0.32\frac{x_{Ni}}{x_W} = \frac{w_W 0.32 x_{Ni}}{1 - 0.01 - x_{Ni}}$$

The amorphous nature of the Ni–W–B alloys deposited under differing conditions employed here was verified by X-ray diffraction. The uniform absence of diffraction peaks shows that the deposits are amorphous, in accordance with other studies of this alloy [14].

All chemicals for the bath were obtained from Amorphous Metals Technologies, Inc. Ion exchanged water was passed through a four-cartridge Millipore Milli-Q purification system; this water was used for preparation of all solutions. Purified argon was used for deoxygenating.

3. Results and discussion

3.1. *Cyclic voltammetry*

Figure 1 shows cyclic voltammograms on the glassy carbon RDE in deoxygenated solution.

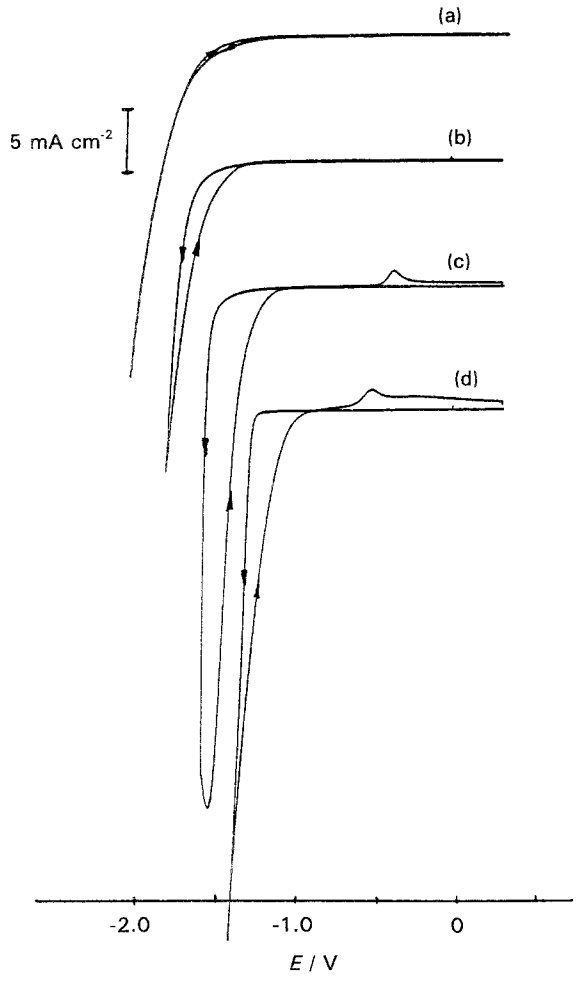

Fig. 1. Cyclic voltammograms on glassy carbon disc electrode in deoxygenated solution of: (a) 0.244 M $(Na)_2Cit.$ + 0.417 M $(NH_4)_2SO_4$ + 45.5 mM BPO_4, pH 8.5; (b) (a) + 0.234 M Na_2WO_4; (c) (a) + 0.025 M $NiSO_4$; (d) (b) + 0.025 M $NiSO_4$. Scan rate 50 mV s^{-1}, rotation rate 1000 rpm.

Voltammogram (a) of Fig. 1 shows that the hydrogen evolution process starts around −1.6 V vs SCE in the solution of sodium citrate, ammonium sulfate and boron phosphate.

Voltammograms (b)–(d) of Fig. 1 were obtained in solutions containing tungsten (voltammogram (b)), nickel (voltammogram (c)) and both nickel and tungsten (voltammogram (d)). In each of these cases, the current after sweep reversal crosses over the current on the forward scan, which suggests changes of the electrode surface. The cathodic reaction begins at more positive potential when nickel is present, 250 mV more positive in voltammogram (c) and 400 mV more positive in voltammogram (d). In the presence of nickel (c) or both metals (d) stripping peaks are observed. Anodic peaks on voltammograms (c) and (d) suggest electrodeposition of a metallic phase on the glassy carbon electrode. The anodic peak is shifted to more negative potential by 150 mV and the shape of the anodic peak is changed in voltammogram (d) in comparison with voltammogram (c). Results of analysis of the deposited alloy according to the procedure described in the experimental section suggest that the deposit is nickel under

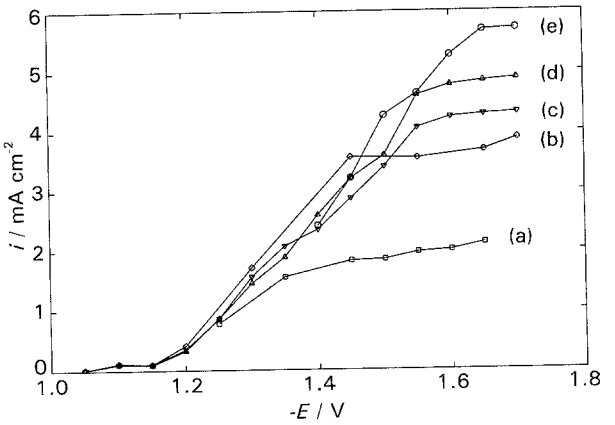

Fig. 2. Partial polarization curves of nickel deposition. Solution: 0.244 M $(Na)_2Cit.$ + 0.417 M$(NH_4)_2SO_4$ + 0.025 M $NiSO_4$. Rotation rate: (a) 500, (b) 1000, (c) 1500, (d) 2000 and (e) 3000 rpm.

conditions of voltammogram (c) and that it is the Ni–W–B alloy for voltammogram (d).

3.2. *Partial polarization curves*

The first series of partial polarization curves was obtained in deoxygenated solution containing sodium citrate, ammonium sulfate and nickel sulfate (pH 8.5).

Partial polarization curves of the hydrogen evolution reaction do not depend significantly on rotation rate of the electrode. This fact indicates that the hydrogen evolution reaction in this solution is controlled mainly by kinetics.

Partial polarization curves for deposition of nickel are shown in Fig. 2. They indicate that the reduction of Ni(II) occurs with diffusion limitation at potentials more negative than −1.4 V. The limiting current increases linearly with increasing square root of the rotation speed, as shown in curve (a) of Fig. 3. The value of diffusion coefficient calculated from the slope of the Levich plot is 5.4×10^{-6} cm^2 s^{-1}, close to the value of the Ni(II) diffusion coefficient in a similar solution (5.56×10^{-6} cm^2 s^{-1}, for the Ni(II) diffusion coefficient in the solution containing 1 M NH_4OH and 3 M NH_4Cl) [15].

A second series of partial polarization curves was obtained in the same solution with addition of

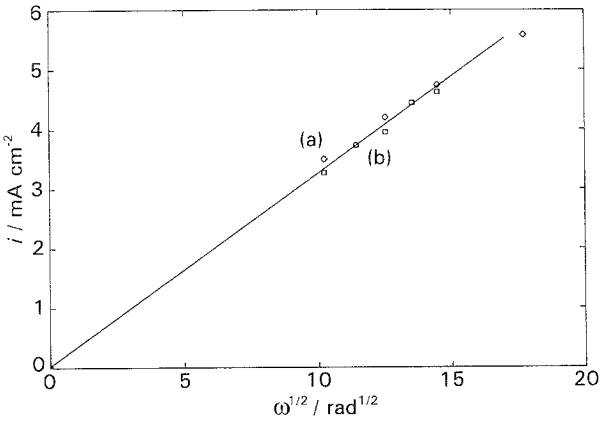

Fig. 3. Levich plots for the nickel partial polarization curves. Solutions: (a, ◇) as in Fig. 2; (b, □) as in Fig. 2 with the addition of 0.234 M Na_2WO_4.

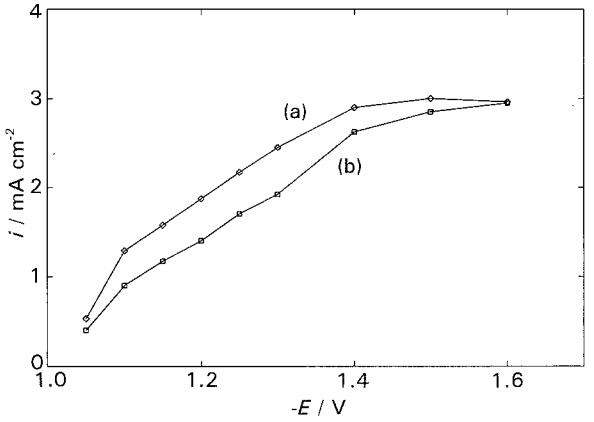

Fig. 4. Partial polarization curves for reduction of W (a, ◇) and Ni (b, □). Solution as in Fig. 3, curve (b). Rotation rate 1000 rpm.

0.234 M sodium tungstate. Results of the analysis of the deposits in this case indicates that the Ni–W alloy was deposited. Typical partial polarization curves are displayed in Fig. 4. Current–potential responses for the hydrogen evolution reaction are also independent of rotation rate in this case.

Partial currents for the deposition of nickel as a component of the alloy have a limiting current plateau for potentials more negative than −1.4 V. A Levich plot for the reduction of Ni(II) to form the alloy is shown in Fig. 3, curve (b). The diffusion coefficient calculated from the slope of this plot is very close to the diffusion coefficient for the reduction of Ni(II) to form the pure phase (5.2×10^{-6} and 5.4×10^{-6} cm^2 s^{-1}, respectively). Thus the deposition of nickel as a pure metal and as a component of the alloy occurs with diffusion limitation in both cases.

Figure 4 also shows a limiting current for deposition of tungsten. This limiting current cannot be due to diffusion limitation in the solution phase, because the concentration of tungsten in the solution is in an order of magnitude greater than the concentration of Ni(II). Moreover, the composition of the alloy is approximately independent of deposition potential, as shown in Table 1. Constant concentration of the alloy components of around 50% w/w for each component is observed at any deposition potential. This can be explained by the stoichiometry of the alloy. The equilibrium phase diagram of the Ni–W alloy [16] indicates that Ni–W solid solution extends up to 45 wt % of tungsten. Tungsten-rich alloys have to include at least three solid phases, solid solution phase and phases of metallic nickel and tungsten. However, tungsten cannot be deposited as a pure metal from aqueous solution. Thus tungsten is only deposited together with nickel to form the alloy. It has to be noted that nonequilibrium phases are formed very often during electrocrystallization process. Probably the supersaturated solid solution is formed at any deposition potential and the limited current of the tungsten deposition is due to the stoichiometric limitations imposed by the alloy.

Table 1. Nickel content in the Ni–W–B alloy (weight percent) as a function of the deposition potential

−E/V	w_{Ni}/wt %
1.10	47.9
1.15	47.1
1.20	46.6
1.25	47.0
1.30	44.5
1.40	45.6
1.50	45.4
1.60	48.4

3.3. *Plating in the steel cell*

The main goal of the plating experiments was to verify the plating parameters of the bath and to explore ways of enhancing the current efficiency.

A series of experiments was performed in the steel cell to determine stability of the bath and plating characteristics. The body of the cell can be used as an anode, because it is known that steel is passivated in alkali solution by a conducting oxide film that forms on the iron surface. The ratio of the anode to cathode areas is almost 300. This leads to very low anode current density. In this case, the anodic current density required to oxidize the electrolyte is not reached, and organic components of the plating bath are stable [17].

Note that the addition of boron phosphate to the solution produces an amorphous alloy, whereas the Ni–W alloy is crystalline.

Figure 5 shows the dependence of current efficiency (curve (a)) and of concentration of nickel in the deposited alloy (curve (b)) on the current density. The current efficiency decreased from 29 to 12% when the current density increased from 45 to 80 mA cm^{-2}. At the same time the nickel concentration in the deposit remained approximately constant.

The minimal effect of current density on composition of the alloy suggests that the mechanism of deposition, complex as it must be, remains substantially the same over this range of current density. The main effect of higher density is lower current efficiency, probably due to increased rate of hydrogen evolution. Both of these observations are consistent

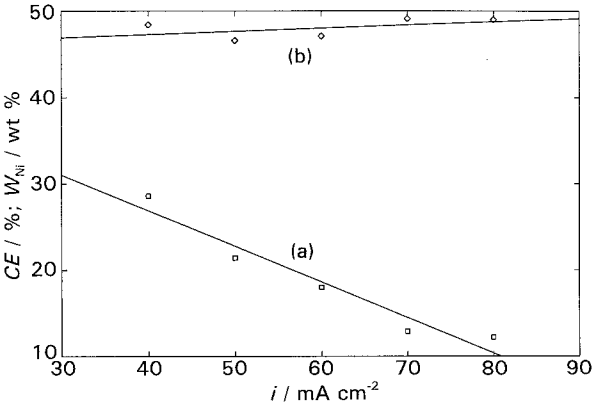

Fig. 5. Current efficiency (CE) (a, □), and Ni concentration in the alloy (W_{Ni}, wt %) (b, ◇) as a function of current density (i). Plating bath with pH 8.5, t = 60 °C.

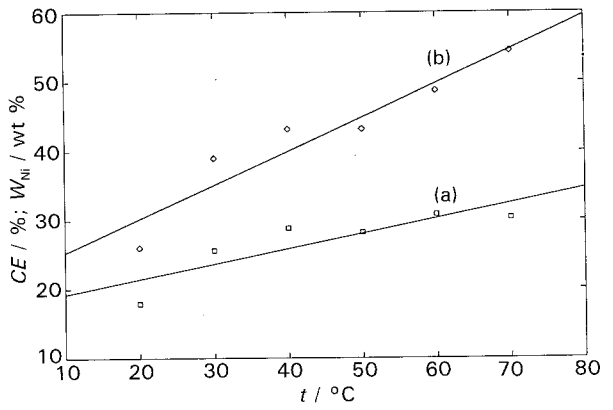

Fig. 6. Current efficiency (CE) (a, □), and Ni concentration in the alloy (W_{Ni}, wt %) (b, ◇) as a function of the temperature. Plating bath with pH 8.5, $i = 45\,mA\,cm^{-2}$.

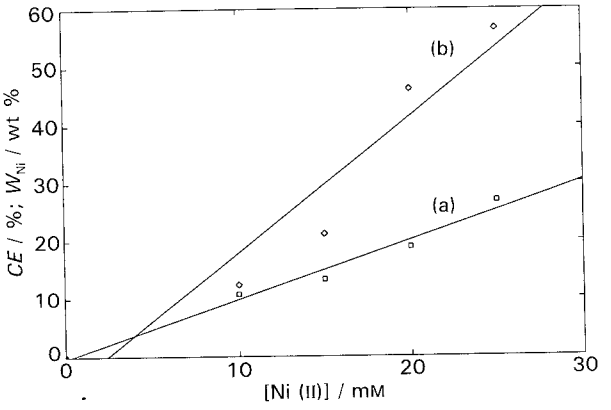

Fig. 7. Current efficiency (CE) (a, □), and Ni concentration in the alloy (W_{Ni}, wt %) (b, ◇) as a function of Ni(II) concentration in the plating bath. Plating bath with pH 8.5, $i = 45\,mA\,cm^{-2}$, $t = 60\,°C$.

with the effect of increased current density being solely that of more negative potential. On the basis of the results of Fig. 5, a current density of 45–50 $mA\,cm^{-2}$ was selected for subsequent experiments.

Figure 6 presents the dependence of current efficiency (curve (a)) and concentration of nickel in the alloy (curve (b)) on temperature. Increasing the temperature increases both the concentration of nickel in the solid phase and the current efficiency. Temperature influences transport properties and kinetic and thermodynamic properties of the charge transfer and the electrocrystallization reaction. The increasing nickel content of the alloy with increasing temperature suggests that the most important effects in this system are the change in overvoltage for tungsten and nickel deposition ($dE^0/dT = -1.36 \times 10^{-3}\,V\,K^{-1}$ for tungsten and $dE^0/dT = 0.06 \times 10^{-3}\,V\,K^{-1}$ for nickel [18]), and the change in viscosity and diffusion coefficients. Improved current efficiency may be due to greater overpotential for reduction of hydrogen ion on nickel than on tungsten. We return to the latter point in Section 3.4. Moreover, increasing the temperature improves the quality of the deposit. Thus, the Ni–W–B deposit started cracking after one hour of plating at 20 °C. At 60 °C cracks did not appear even after a period of more than 3 h. Temperatures in the range 60–70 °C can be used for the working bath. Higher temperatures increase the problem of loss of the volatile components of the bath.

Dependence of current efficiency (curve (a)) and concentration of nickel in the alloy (curve (b)) on the Ni(II) concentration in the solution is given in Fig. 7. The nickel content of the deposit increases with increasing the Ni(II) concentration in solution in the intermediate range, changing from 11 to 55% for concentration of Ni(II) from 10 to 25 mM. Further increases of the Ni(II) concentration is not expedient because high Ni concentration in the deposit leads to changes in the physico-mechanical properties of the alloy. Consequently, the best Ni(II) concentration is between 20 and 25 mM.

The pH of the electrolyte changes during use. The passage of $3\,A\,h\,dm^{-3}$ of electricity reduces the pH from 8.5 to 7.55. Reduction of the pH, in turn, leads to a change in the bath composition and reaction parameters. For example, after passing $3\,A\,h\,dm^{-3}$ through a solution, the colour changes from deep to pale blue. This suggests a decrease in the concentration of ammonia complexes of Ni(II), which have a deep blue colour. The current efficiency also decreases as pH decreases. Considering that the current goes mainly to production of hydrogen, this is not surprising.

3.4. *Pulsed galvanostatic plating*

On the one hand, Figs 6 and 7 indicate that the metal concentration in the alloy depends on the parameters of electrolysis. On the other hand, the rate of hydrogen evolution depends on the alloy composition, because the overvoltage of this reaction is higher for nickel than for tungsten. Even though nickel and tungsten are neighbours in the catalytic activity scale for hydrogen, there are data [19] which suggest a very low overvoltage for the hydrogen evolution reaction on tungsten (for the Tafel equation, $\eta = a + b \log i$, $a = 0.23\,V$ and $b = 0.04\,V$). Moreover, tungsten cannot be deposited from aqueous solution, because overvoltage of hydrogen evolution on the surface of tungsten is very low (after deposition of a thin layer of tungsten, practically only hydrogen is evolved on the cathode) [17, 20, 21]. It is reasonable to hypothesize that hydrogen evolution is preferred on an alloy with high concentration of tungsten, and thus in this case the current efficiency is low. This is consistent with the result of Figs 6 and 7. In this situation, current steps designed to increase the average surface concentration of nickel in the alloy could increase the current efficiency.

A series of experiments was performed at constant current with a current–time profile of an unsymmetrical square wave of period τ and constant average current density $i_a = 45\,mA\,cm^{-2}$. The current density for the first part of the period is $i_1 = 10\,mA\,cm^{-2}$ for time $\Theta_1\tau$. During the second part of the period, time $\Theta_2\tau$, the current density is $i_2 = (i_a - \Theta_1 i_1)/\Theta_2$.

Using this kind of current-time control makes it

possible to obtain deposits with a high nickel concentration during the first step (Θ_1) and deposits with high tungsten concentration during the second step (Θ_2). This can be caused by the rapid depletion of the Ni(II) concentration in the vicinity of the electrode during the second (high current density) step. The decrease of the Ni(II) concentration in the solution, in turn, leads to decreasing the nickel content in the alloy (Fig. 6). Changing Θ_1 and Θ_2 makes it possible to keep a constant average current density. In these experiments, i_2 varied from 80 to 360 mA cm^{-2}. The fraction Θ_1 was changed over the range 0.9–0.5.

Figure 8 shows the dependence of current efficiency and concentration of nickel in the alloy on the ratio of times Θ_2/Θ_1. Increase of Θ_2/Θ_1 increases current efficiency and decreases the concentration of nickel in the alloy. The current efficiency and nickel content in the alloy decrease exponentially with increasing of the amplitude of the second step (i_2) of the current density. The best result (current efficiency 32%) was obtained for $\Theta_1/\Theta_2 = 1$, $\tau = 1$ s, $i_2 = 80$ mA cm^{-2}. In this series of experiments, periods of about 1 s were used. Using other current–time profiles makes it possible to increase the average current density at the same current efficiency. For example, deposits of high quality were obtained for $\tau = 2.2$ s, $\Theta_1 = 0.1$, $\Theta_2 = 0.9$, $i_1 = 0$, $i_2 = 100$ mA cm^{-2}, $i_a = 90$ mA cm^{-2}. The current efficiency was 20%.

3.5. *Maintaining constant concentration of Ni(II) during electrolysis*

The results of Fig. 7 make clear that it is critical to maintain constant the concentration of Ni(II) in the plating bath during electrolysis. Because the molar ratio of Ni to W in the alloy is about 30 times greater than in the bath, the bath is quickly depleted of nickel if some steps are not taken to buffer the nickel concentration.

Bipolar electrodes are used in certain industrial processes (e.g., in hydrometallurgy). The metal electrode is put at open circuit between the anode and cathode in the solution. In this case, there is a cathodic process on the side of the bipolar electrode turned to the anode, and there is an anodic process on the other side. A nickel bipolar electrode can be used in the Ni–W–B alloy plating process. During the reactions, one side of the bipolar electrode (cathode) will be plated by the alloy, the other side (anode) will dissolve.

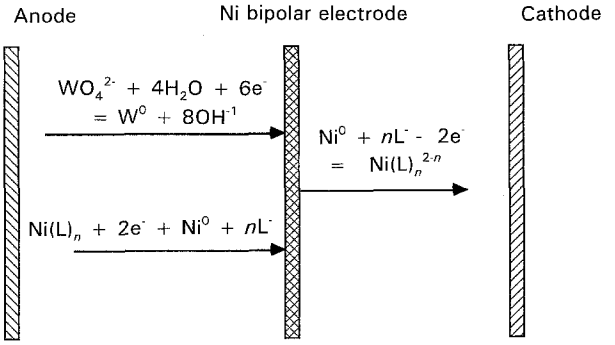

Fig. 9. The principal scheme of the workings of the nickel bipolar electrode.

Figure 9 shows the principal scheme of the nickel bipolar electrode. The anodic current efficiency in the Ni–W–B alloy plating process is larger than the cathodic current efficiency. Consequently, the Ni(II) concentration in the solution must increase. Moreover, there are two reactions in the cathodic process and one reaction in the anodic process. This fact allows for control of the relative current efficiency by several means.

The first set of experiments with a bipolar electrode was performed in the steel cell. A special cathode was designed to give cylindrical geometry. The Ni(II) concentration stays approximately constant when the bipolar electrode is used under these conditions of optimal geometry.

The second set of experiments was performed in the 2 dm^3 glass bath with anode compartment. The Ni(II) concentration in the solution decreases with time, as shown in Fig. 10, curve (a). At the same time, the pH increases from 8.5 to 8.8, because hydrogen is evolved on the cathode.

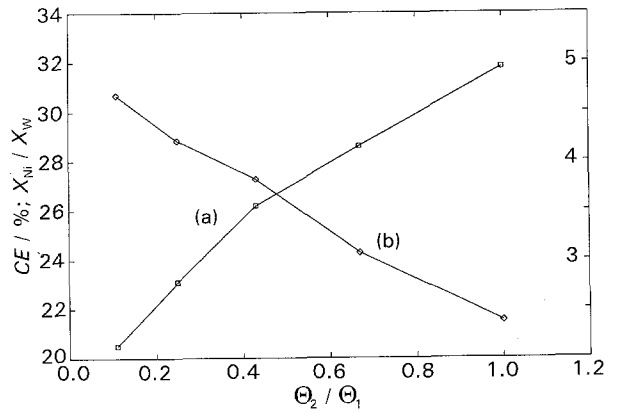

Fig. 8. Current efficiency (CE) (□) and the ratio of Ni and W concentrations (mole fractions) (◇) in the alloy as a function of ratio of the step times. Plating bath with pH 8.5. Current time profile: $\tau = 1$ s, $i_1 = 10$ mA cm^{-2}, $i_{av} = 45$ mA cm^{-2}, $i_{av} = \Theta_1 i_1 + \Theta_2 i_2$.

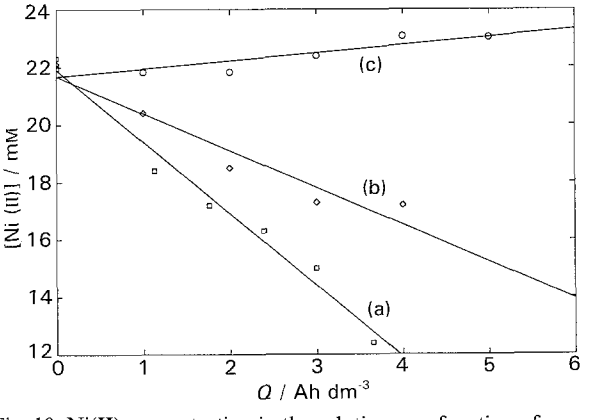

Fig. 10. Ni(II) concentration in the solution as a function of quantity of electricity (Q) (2 dm^3 cell, anode compartment). Solution: plating bath (a, b), plating bath + 0.1 M NH_4Cl (c). Bath with bipolar electrode (b, c). pH = 8.5, current density = 45 mA cm^{-2}, $T = 60$ °C.

A bipolar electrode from nickel foil (0.785 mm thick) was placed between the cathode and the anode compartment. In this case, the concentration of Ni(II) in the solution decreases, even when the bipolar electrode is used, albeit at a lesser rate. The typical result is shown in Fig. 10, curve (b). The less favourable result (in comparison with that from the stainless steel cell) is due to the unfavourable cell geometry.

There are two ways to activate the anodic process of the bipolar electrode. Almost all nickel plating solutions contain chloride. Chloride activates the anodic dissolution of metallic nickel. When chloride (0.1 M NH_4Cl) is added to the solution for Ni–W–B plating, the concentration of Ni(II) decreases less rapidly during the plating process than in the solution without chloride.

Changes of the current density on the bipolar electrode lead to changing parallel reaction rates. Experiments with bipolar electrodes described above were performed with ratio of the anode to the cathode areas of 5 : 1. Decreasing the area of the bipolar electrode increases the anodic and cathodic current density on the bipolar electrode. The best ratio of areas was found to be 3 : 1. In this case, the concentration of Ni(II) and the pH are approximately constant in the solution containing chloride. This result is demonstrated in curve (c) of Fig. 10. Further reduction of the area (to 1 : 1) of the bipolar electrode passivates the anodic side of the electrode (salt passivation).

Conclusions

(i) Partial polarization curves for deposition of nickel as a pure metal and as a component of the Ni–W alloy show that reduction of Ni(II) is diffusion-controlled in both cases; the value of diffusion coefficient for Ni(II) in this medium is $(5.3 \pm 0.1) \times 10^{-6}\,cm^2\,s^{-1}$.

(ii) The deposition of tungsten as a component of the Ni–W alloy from citrate solution is limited by the stoichiometry of the alloy. The rate of deposition of tungsten is determined by the rate of deposition of nickel because the concentration of tungsten in the solid phase cannot exceed 50–55 wt %.

(iii) The optimal ranges for parameters of the plating process were found to be current density 45–50 mA cm^{-2}, temperature 60–70 °C, Ni(II) concentration 20–25 mM and pH 8.5.

(iv) Pulsed plating increased slightly the current efficiency. For example, at 45 mA cm^{-2}, the current efficiency increased from 25 to 31% on applying a symmetrical galvanostatic squarewave with $i_1 = 10$ and $i_2 = 80\,mA\,cm^{-2}$.

(v) Employing a nickel bipolar electrode is an effective method for self-regulation of Ni(II) in the solution during electroplating. Difference in the anodic and cathodic current efficiency leads to net production of Ni(II). The rate of production increases with increasing current density on the bipolar electrode and with addition of chloride to the bath.

Acknowledgements

This work was supported in part by Amorphous Metals Technologies Inc. The authors thank Louise Mahoney for technical assistance.

References

[1] W. Klement Jr., R. H. Willens and P. Duwez, *Nature (UK)* **187** (1960) 869.
[2] Yu. M. Polukarov and V. V. Bondar, *Dokl. Akad. Nauk SSSR* **123** (1958) 720.
[3] A. Szasz, D. J. Fabian, Z. Paal and J. Kojnok, *J. Non Cryst. Solids* **103** (1988) 21.
[4] Y. Akahama, Y. Mori, M. Kobayashi, H. Kawamura, K. Kimura and S. Takeuchi, *J. Rhys. Soc. Jpn.* **58** (1989) 2231.
[5] V. M. Knyazheva, E. A. Ul'ianin and L. A. Yanov, Itogi Nauki, Tekh. *Ser. Korroz. Zashch. Korroz.* **9** (1982) 225.
[6] M. Naka, K. Hashimoto, K. Asami and T. Masumoto, *in* 'Rapidly quenched metals', (edited by B. Cantor), Proc. Int. Conf. 3rd Met. Soc., London, vol. 2 (1978) p. 449.
[7] C. A. Pampillo, *J. Mater. Sci.* **10** (1975) 1194.
[8] G. A. Croopnik and D. M. Scruggs, *US Patent 4529668* (16 July 1985).
[9] M. Donten and J. Osteryoung, *J. Appl. Electrochem.* **21** (1991) 496.
[10] K. Wikiel and J. Osteryoung, *ibid.* **22** (1992) 506.
[11] M. Donten, Z. Stojek and J. Osteryoung, *J. Electrochem. Soc.* **140** (1993) 3417.
[12] E. Chassing, K. Vu Quang and R. Wiart, *J. Appl. Electrochem.* **18** (1989) 839.
[13] R. Wiart, *Electrochim. Acta* **35** (1990) 1587.
[14] Private communication, Amorphous metals Technologies, Inc.
[15] I. M. Kolthoff and J. J. Lingne, 'Polarography', Interscience Publishers, New York (1965), p. 487.
[16] M. Hancen, 'Constitution of binary alloys' McGraw-Hill, New York (1958), p. 1057.
[17] S. Grilikhes and K. Tikhonov, 'Electrolytic and electroless deposits' (in Russian), Chemistry, Leningrad (1990), p. 288.
[18] A. Rotinian, K. Tikhonov and I. Shoshina, 'Theoretical electrochemistry' (in Russian), Chemistry, Leningrad (1981) p. 160.
[19] J. Bockris and R. Parsons, *Trans. Faraday Soc.* **44** (1948) 860.
[20] A. Brenner, 'Electrodeposition of alloys', Academic Press, New York and London, vol. 2 (1963), p. 429.
[21] T. Alekhina, I. Shoshina, B. Karbasov, *Russian J. Electrochem.* **30** (1994) 241.